Optical Detection of Submicromolar level Nitro Explosives by a Submicron sized Metal-Organic Phosphor Material

Debal Kanti Singha,[a] Saurav Bhattacharya,[b] Prakash Majee,[c] Sudip Kumar Mondal,*[c] Manoranjan Kumar,[a] and Partha Mahata*[a]

[a]Department of Condensed Matter Physics and Material Sciences, S.N Bose National Centre for Basic Sciences, JD Block, Sector III, Salt Lake City, Kolkata -700098, India. Email: partha.mahata@bose.res.in

[b]Framework solids Laboratory, Solid State and Structural Chemistry Unit, Indian Institute of Science, Bangalore-560012, India.

[c]Department of Chemistry, Siksha-Bhavana, Visva-Bharati University, Santiniketan-731235, West Bengal, India. Email: sudip.mondal@visva-bharati.ac.in

ELECTRONIC SUPPLEMENTARY INFORMATION

Table S1: Crystal data and structure refinement parameters for $[Y_2\{C_8H_8(COO)_2\}_3(H_2O)]\cdot 2H_2O$, **1**.

Empirical formula	$C_{30}H_{30}O_{15}Y_2$
Formula weight	808.36
Crystal system	Monoclinic
Space group	$P2_1/c$ (no. 14)
a (Å)	21.625(3)
b (Å)	10.0060(13)
c (Å)	14.0570(17)
α (deg)	90.0
β (deg)	91.401(7)
γ (deg)	90.0
Volume ($Å^3$)	3040.8(6)
Z	4
T (K)	293(2)
ρ_{calc} ($g\ cm^{-3}$)	1.766
μ (mm^{-1})	3.874
θ range (deg)	1.88 to 27.63
λ (Mo Kα) (Å)	0.71073
R indices [I>2σ(I)]	$R_1 = 0.0462$, $wR_2 = 0.0815$
R indices (all data)	$R_1 = 0.0905$, $wR_2 = 0.0940$

$R_1 = \Sigma\ ||F_0|-|F_c|| / \Sigma\ |F_0|$; $wR_2 = \{\Sigma[w(F_0^2 - F_c^2)^2] / \Sigma[w(F_0^2)^2]\}^{1/2}$. $w = 1/[\sigma^2(F_0)^2 + (aP)^2 + bP]$, $P = [max.(F_0^2,0) + 2(F_c)^2]/3$, where a = 0.0337 and b =0.00.

Table S2: Selected bond distances (Å) observed in $[Y_2\{C_8H_8(COO)_2\}_3(H_2O)]\cdot 2H_2O$, **1**.

Bond	Distances, Å	Bond	Distances, Å
Y(1)-O(9)	2.242(3)	Y(2)-O(10)#3	2.332(2)
Y(1)-O(3)#1	2.280(2)	Y(2)-O(13)	2.357(3)
Y(1)-O(8)#2	2.290(2)	Y(2)-O(12)	2.377(2)
Y(1)-O(6)	2.325(3)	Y(2)-O(2)#3	2.379(3)
Y(1)-O(11)	2.334(2)	Y(2)-O(4)#1	2.402(3)
Y(1)-O(1)	2.364(2)	Y(2)-O(7)#4	2.432(3)
Y(1)-O(12)	2.560(3)	Y(2)-O(8)#4	2.446(2)
Y(1)-O(2)	2.693(3)	Y(2)-O(3)#1	2.666(3)
Y(2)-O(5)	2.312(3)		

Symmetry operations used to generate equivalent atoms: `#1 -x+1,-y+1,-z; #2 -x,-y+2,-z; #3 x,-y+3/2,z+1/2; #4 -x,y-1/2,-z+1/2`

Table S3: Selected bond angles observed in $[Y_2\{C_8H_8(COO)_2\}_3(H_2O)]\cdot 2H_2O$, **1**.

Angle	Amplitude (º)	Angle	Amplitude
O(9)-Y(1)-O(3)#1	80.19(10)	O(11)-Y(1)-O(1)	81.11(10)
O(9)-Y(1)-O(8)#2	82.70(9)	O(9)-Y(1)-O(12)	144.21(8)
O(3)#1-Y(1)-O(8)#2	162.29(9)	O(3)#1-Y(1)-O(12)	66.55(9)
O(9)-Y(1)-O(6)	78.13(11)	O(8)#2-Y(1)-O(12)	131.15(8)
O(3)#1-Y(1)-O(6)	103.50(10)	O(6)-Y(1)-O(12)	96.53(10)
O(8)#2-Y(1)-O(6)	77.20(10)	O(11)-Y(1)-O(12)	52.31(8)
O(9)-Y(1)-O(11)	156.96(10)	O(1)-Y(1)-O(12)	75.86(9)
O(3)#1-Y(1)-O(11)	118.86(9)	O(9)-Y(1)-O(2)	73.07(9)
O(8)#2-Y(1)-O(11)	78.85(9)	O(3)#1-Y(1)-O(2)	103.82(9)
O(6)-Y(1)-O(11)	84.40(11)	O(8)#2-Y(1)-O(2)	66.53(8)
O(9)-Y(1)-O(1)	115.34(10)	O(6)-Y(1)-O(2)	135.76(10)
O(3)#1-Y(1)-O(1)	85.07(9)	O(11)-Y(1)-O(2)	111.21(9)
O(8)#2-Y(1)-O(1)	98.27(10)	O(1)-Y(1)-O(2)	50.35(8)
O(6)-Y(1)-O(1)	165.42(10)	O(12)-Y(1)-O(2)	126.20(8)

Symmetry operations used to generate equivalent atoms: #1 -x+1,-y+1,-z; #2 -x,-y+2,-z

Table S4: Result of optical gap calculation using DFT [Basis set 6-311+g(d,p) using Gaussian 03]#

Compound	Calculated optical gap in terms of energy (eV)	Calculated optical gap in terms of wavelength (nm)	Oscillator strength
Optimized PDA ligand moiety	5.7571	215.36	0.0089
	5.7629	215.14	0.0142
TNP (2,4,6-trinitro phenol)	4.6781	265.03	0.0046
	4.7869	259.01	0.0001
	5.0917	243.5	0.0008
	5.1660	240.0	0.0004
	5.2510	236.12	0.1273
	5.4092	229.21	0.0005
	5.6001	221.40	0.0355
DNB (1,3-dinitro benzene)	5.1052	242.86	0.0008
	5.5259	224.37	0.0309
	5.5393	223.83	0.0361
DNT (2,4-dinitrotoluene)	4.7287	262.20	0.0053
	5.0855	243.80	0.0006
	5.1179	242.25	0.0005
	5.4698	226.67	0.1041
	5.5774	223.30	0.0081
NB (nitro benzene)	5.1024	242.99	0.0004
	5.4858	226.01	0.0277
	5.5084	225.08	0.1134
NT (4-nitro toluene)	5.1266	241.85	0.0004
	5.3890	230.07	0.1886
	5.5134	224.88	0.0169
B (benzene)	7.3318	169.10*	0.0892

*For Benzene, no optical transition is available in more than 200 nm wavelength. Transition corresponds to 169.10 nm is the lowest energy transition.

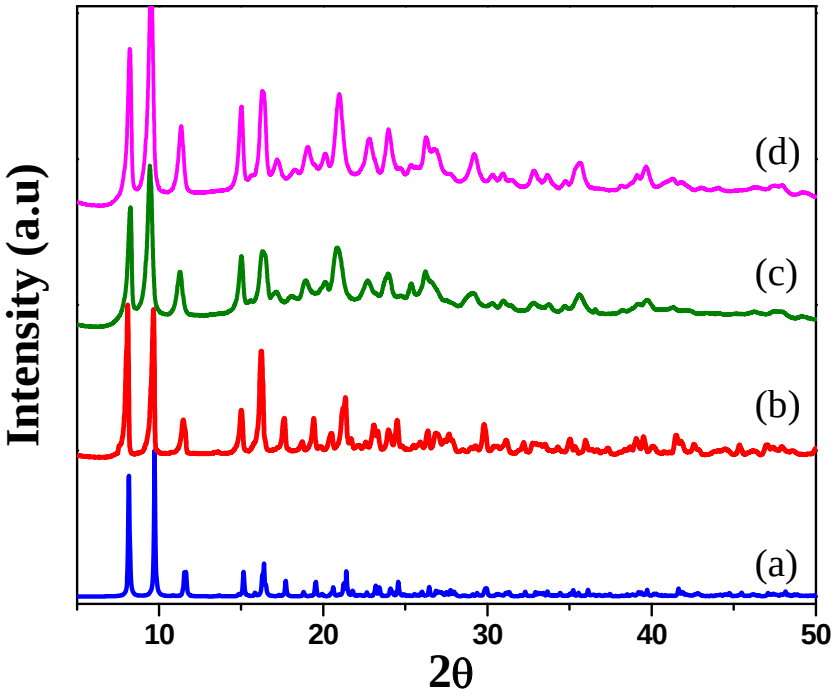

Fig. S1: Powder XRD (CuKα) patterns: (a) simulated from single crystal X-ray data of $Y_2\{C_8H_8(COO)_2\}_3(H_2O)]\cdot 2H_2O$, **1**, (b) solvothermally synthesized bulk **1**, (c) **1**, (d) **Tb@1**.

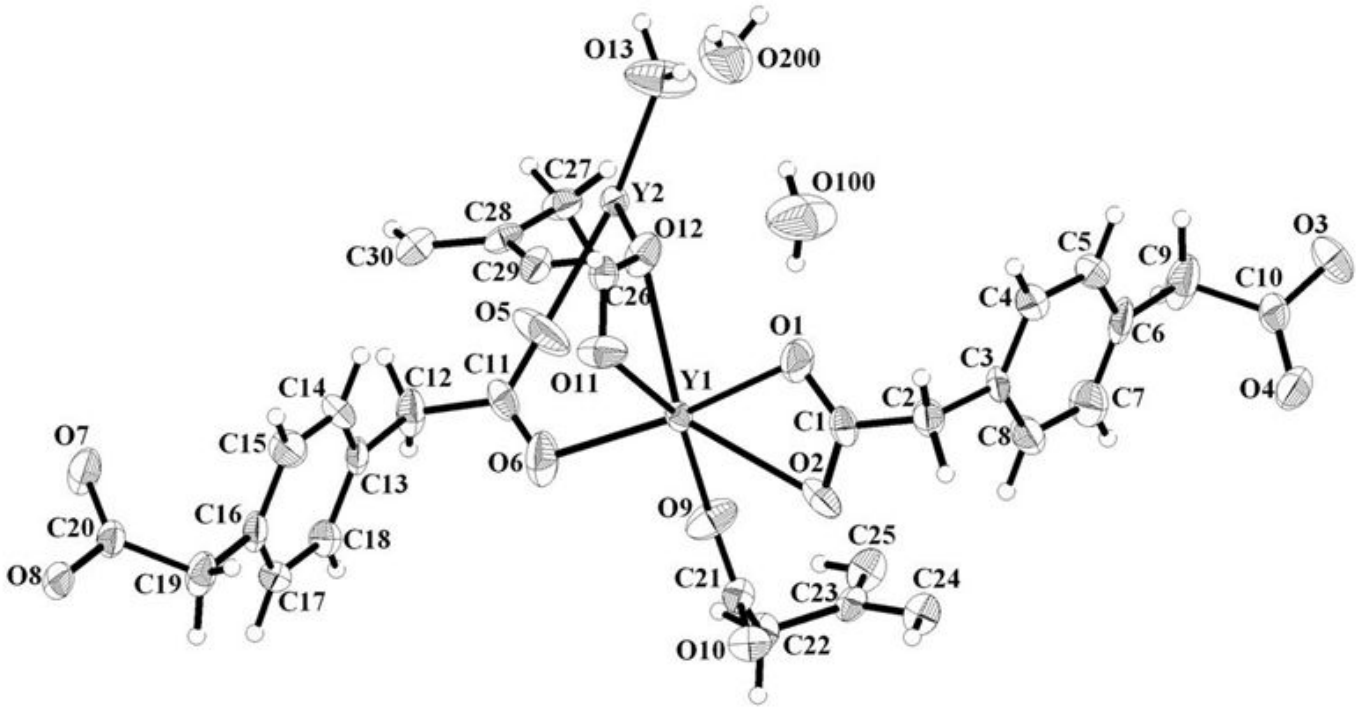

Fig. S2: Figure shows ORTEP* diagram of the asymmetric unit of $Y_2\{C_8H_8(COO)_2\}_3(H_2O)]\cdot 2H_2O$, **1**. Thermal ellipsoids are given at 50% probability. The hydrogen atoms are shown as solid spheres.

(* J. L. Farrugia, *J. Appl. Crystallogr.*, 1997, **30**, 565)

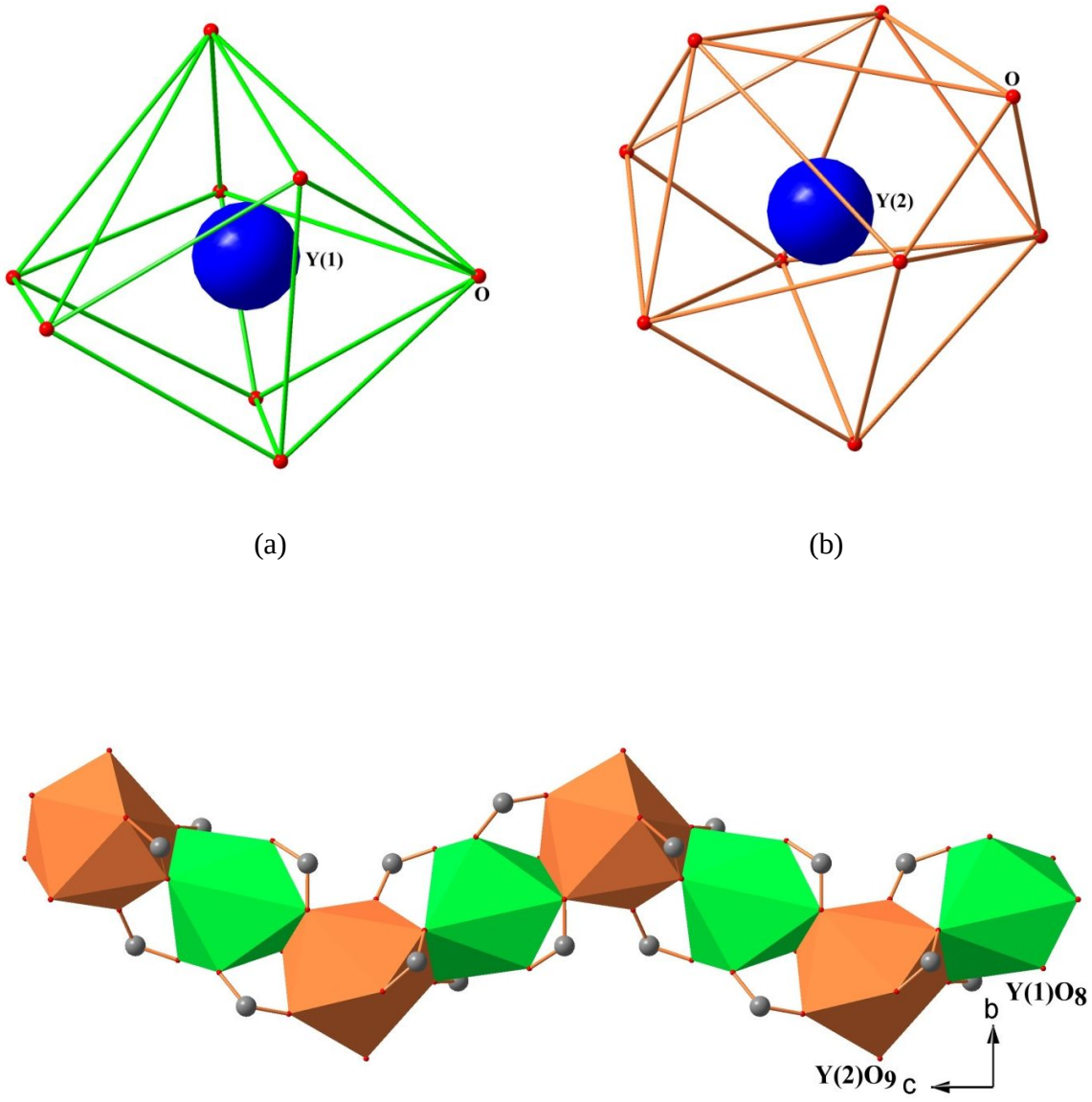

(a) (b)

(c)

Fig. S3: Figure shows the coordination geometries around Y^{3+} metal ions in $[Y_2\{C_8H_8(COO)_2\}_3(H_2O)]\cdot 2H_2O$, **1**: (a) distorted dodecahedron coordination geometry around Y(1) metal ion, (b) distorted tricapped trigonal prismatic geometry around Y(2) metal ion, (c) one-dimensional zigzag metal ions [Y(1) and Y(2)] and carboxylates connected chains parallel to the *c* axis.

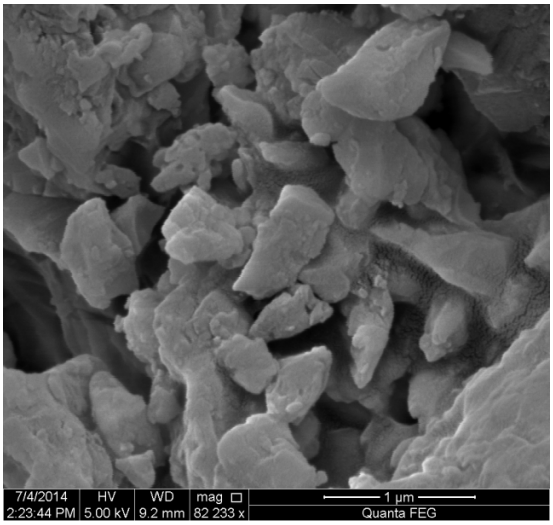

(a)

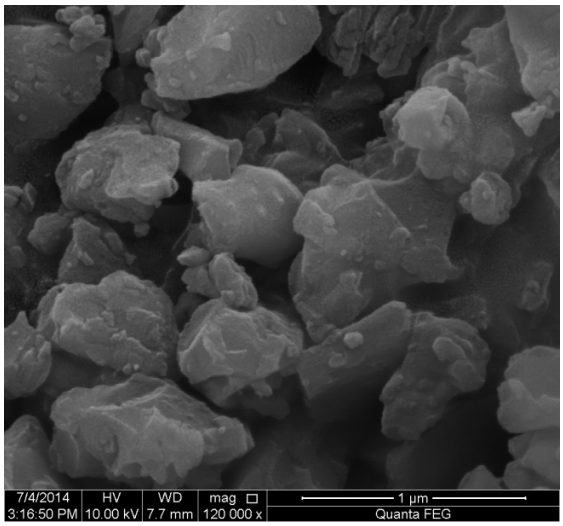

(b)

Fig. S4: SEM images: (a) **1**, and (b) **Tb@1.** Note the size of the particles in submicron regime.

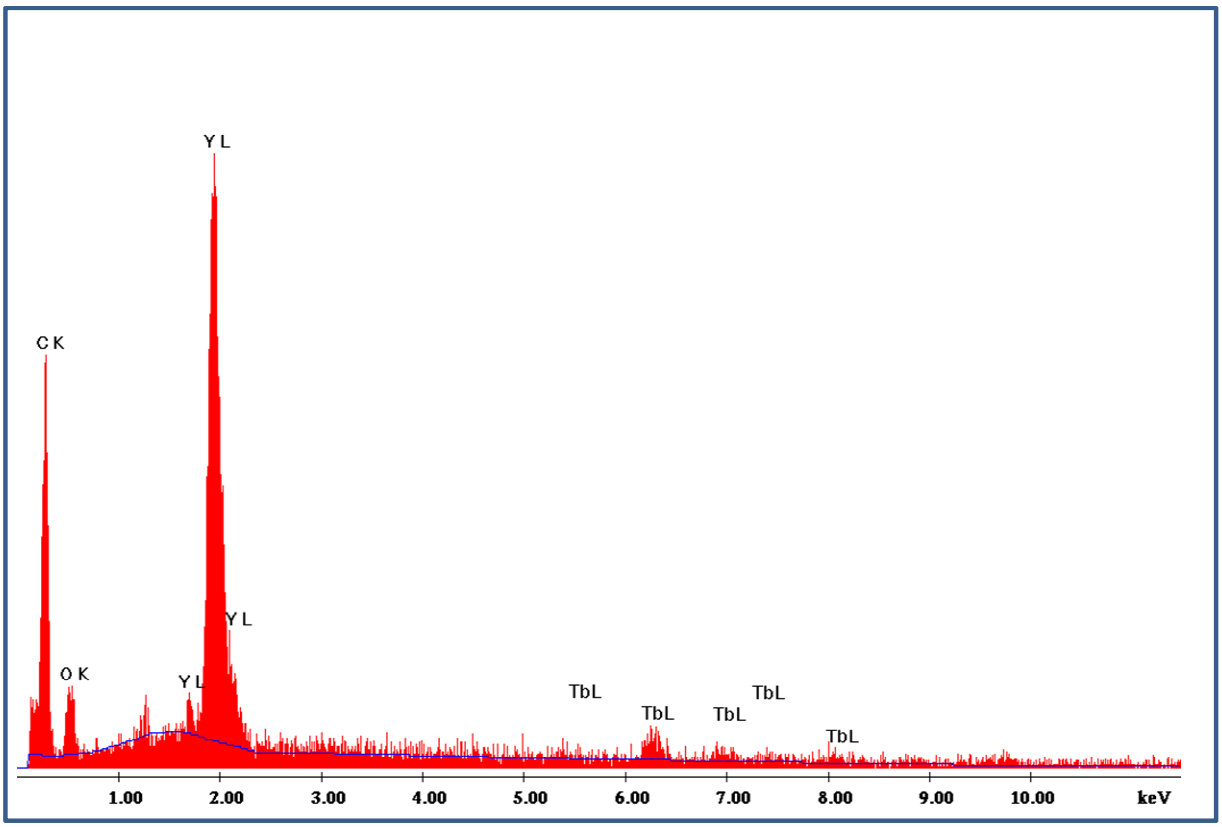

Fig. S5: Representative EDX plot of **Tb@1.** Note the presence of Tb and Y.

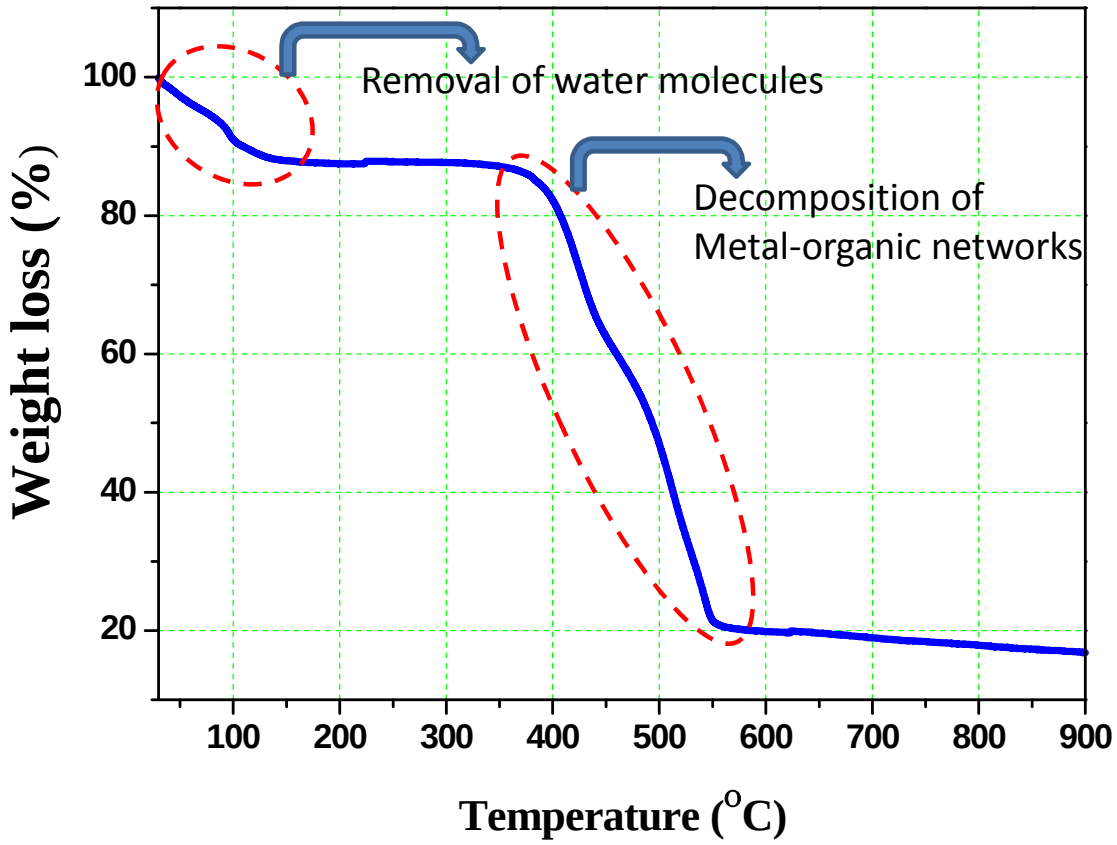

Fig. S6: Thermogravimetric analysis (TGA) of $[Y_2\{C_8H_8(COO)_2\}_3(H_2O)]\cdot 2H_2O$, **1,** in nitrogen atmosphere. Note the stability of the dehydrated compounds upto 350 °C.

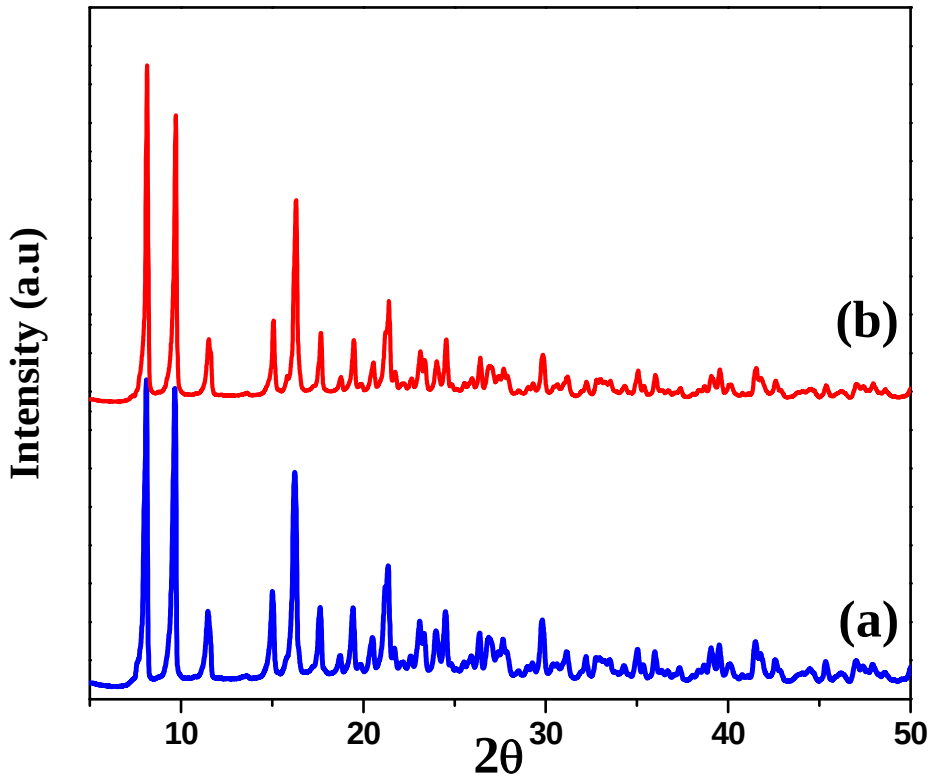

Fig. S7: (a) Powder XRD (CuKα) patterns: (a) **1**, and (b) dehydrated **1** after heating at 200 °C for 2 hrs in hot air oven. Note the similar XRD patterns before and after heating.

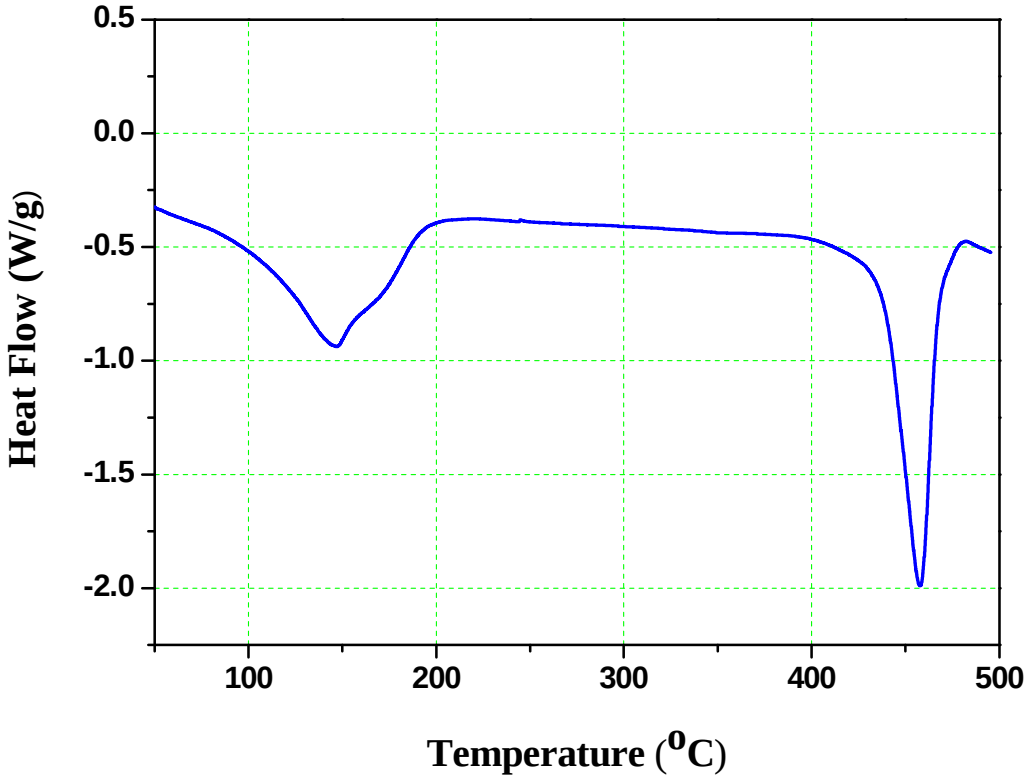

Fig. S8: Differential scanning calorimetry (DSC) study of **1**. Note the two endothermic peaks (removal of water and decomposition of networks).

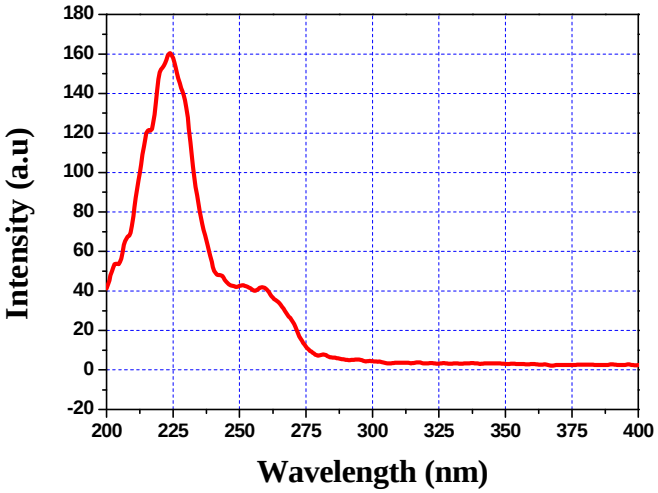

(a)

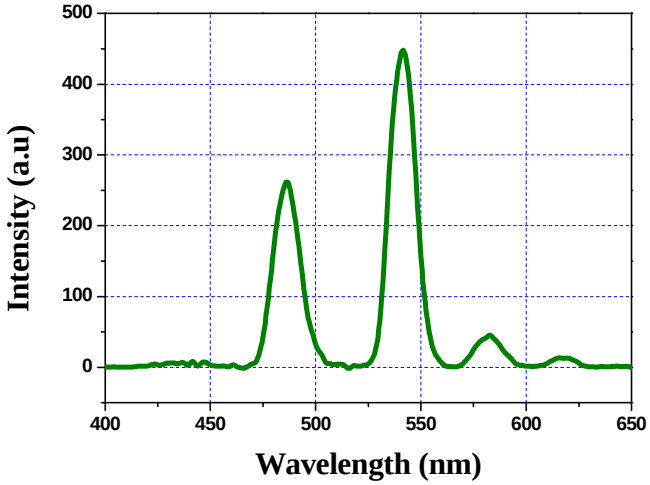

(b)

Fig. S9: (a) Excitation spectra (monitored at λ_{em} = 540 nm) of **Tb@1' (**dehydrated Tb@1**)**, and (b) Emission spectra of **Tb@1'** dispersed in acetonitrile (λ_{ex} = 225 nm, filter: 430 nm cut-off). All the spectra measured using PerkinElmer LS-55 spectrofluorometer. **Tb@1'** suspension in acetonitrile was prepared by sonicating the mixture of grinded **Tb@1'** and acetonitrile for 1 hour.

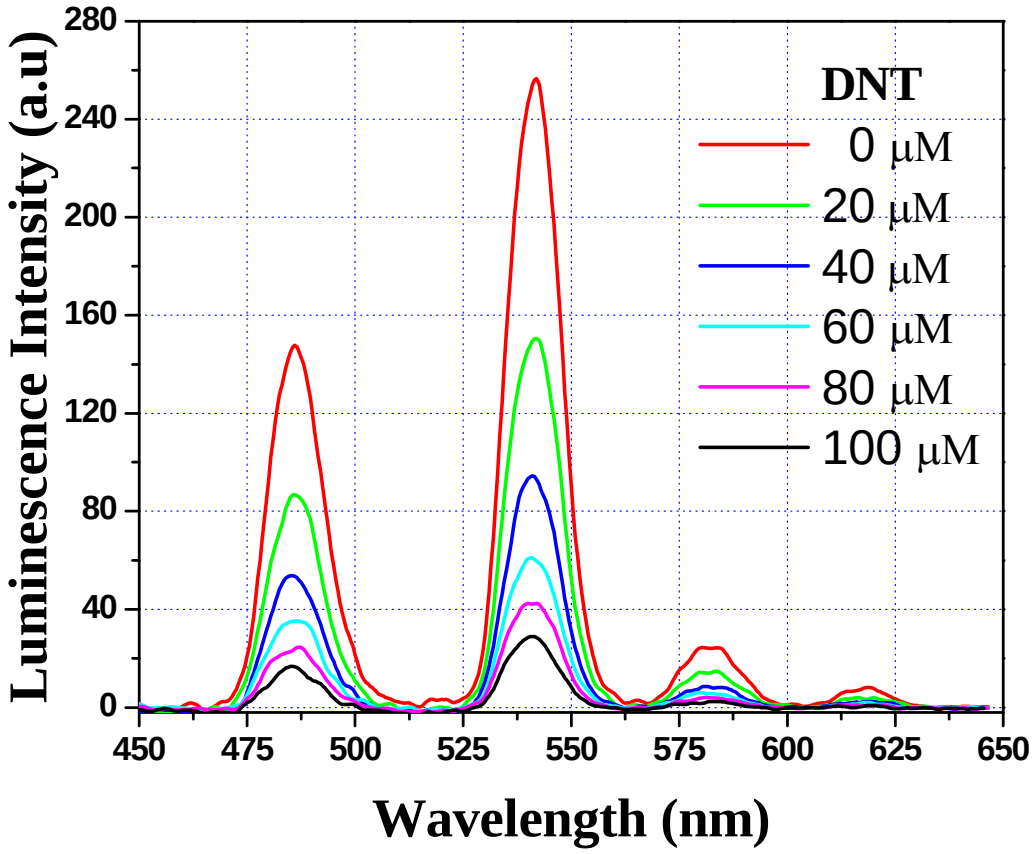

Fig. S10: Emission spectra of **Tb@1'** dispersed in acetonitrile upon incremental addition of DNT solution (λ_{ex} = 225 nm; filter: 430 nm cut-off). The final concentration of DNT in the medium is indicated in the legend. All the spectra are measured using PerkinElmer LS-55 spectrofluorometer. **Tb@1'** suspension in acetonitrile was prepared by sonicating the mixture of grinded **Tb@1'** and acetonitrile for 1 hour.

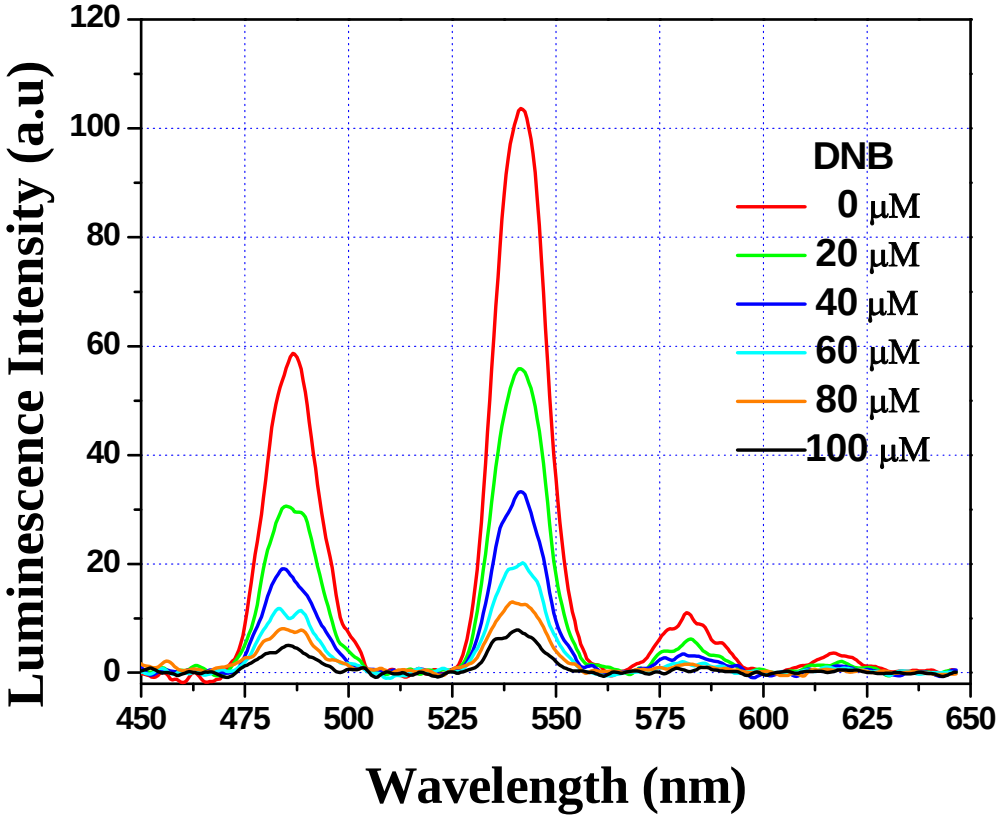

Fig. S11: Emission spectra of **Tb@1'** dispersed in acetonitrile upon incremental addition of DNB solution (λ_{ex} = 225 nm; filter: 430 nm cut-off). The final concentration of DNB in the medium is indicated in the legend. All the spectra are measured using PerkinElmer LS-55 spectrofluorometer. **Tb@1'** suspension in acetonitrile was prepared by sonicating the mixture of grinded **Tb@1'** and acetonitrile for 1 hour.

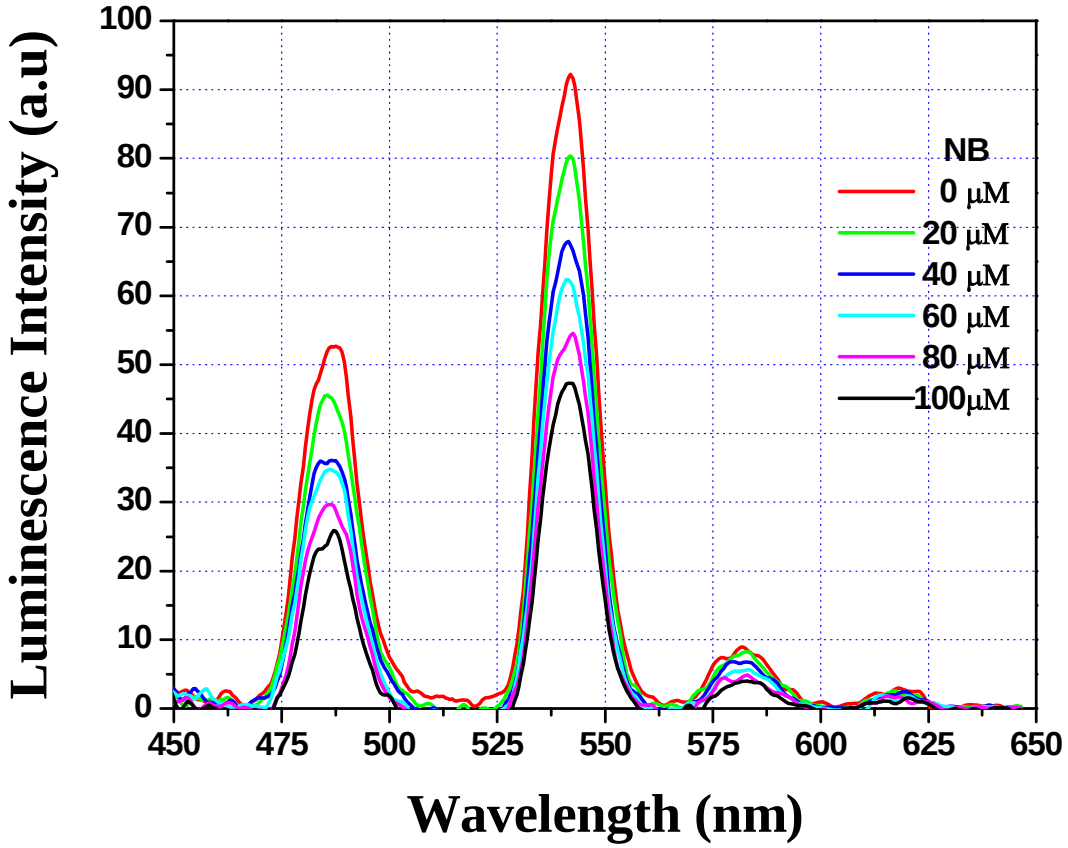

Fig. S12: Emission spectra of **Tb@1'** dispersed in acetonitrile upon incremental addition of NB solution (λ_{ex} = 225 nm; filter: 430 nm cut-off). The final concentration of NB in the medium is indicated in the legend. All the spectra are measured using PerkinElmer LS-55 spectrofluorometer. **Tb@1'** suspension in acetonitrile was prepared by sonicating the mixture of grinded **Tb@1'** and acetonitrile for 1 hour.

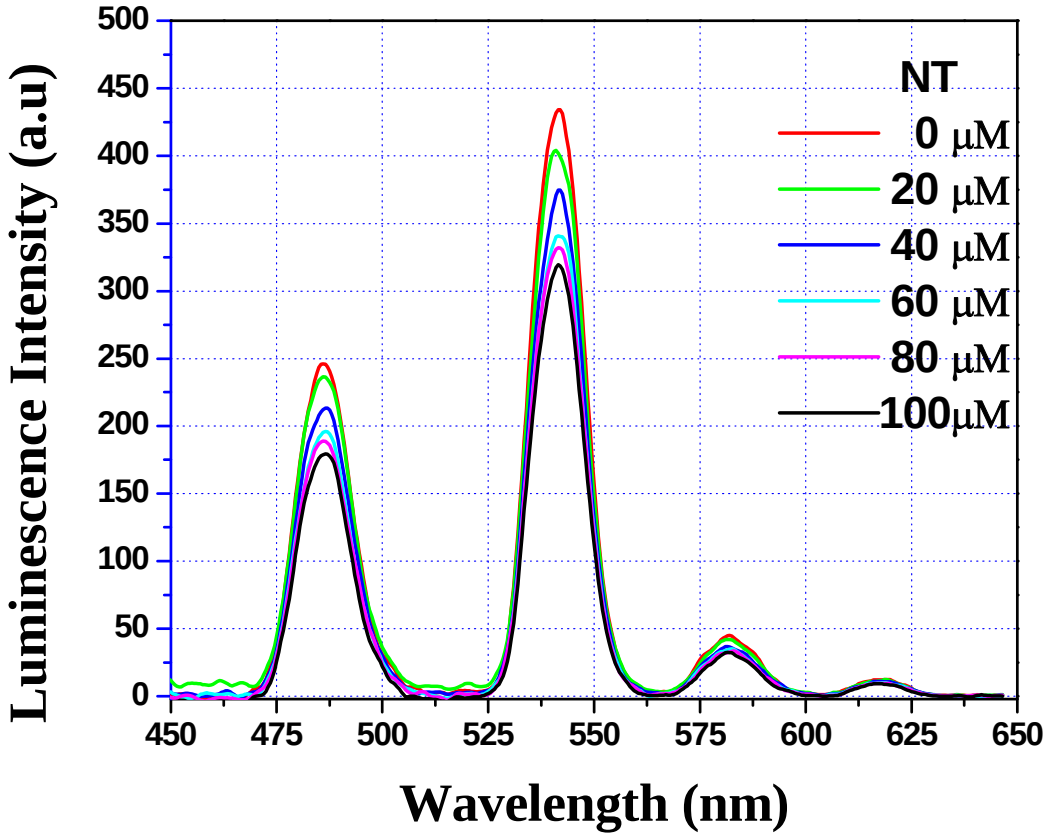

Fig. S13: Emission spectra of **Tb@1'** dispersed in acetonitrile upon incremental addition of NT solution (λ_{ex} = 225 nm; filter: 430 nm cut-off). The final concentration of NT in the medium is indicated in the legend. All the spectra are measured using PerkinElmer LS-55 spectrofluorometer. **Tb@1'** suspension in acetonitrile was prepared by sonicating the mixture of grinded **Tb@1'** and acetonitrile for 1 hour.

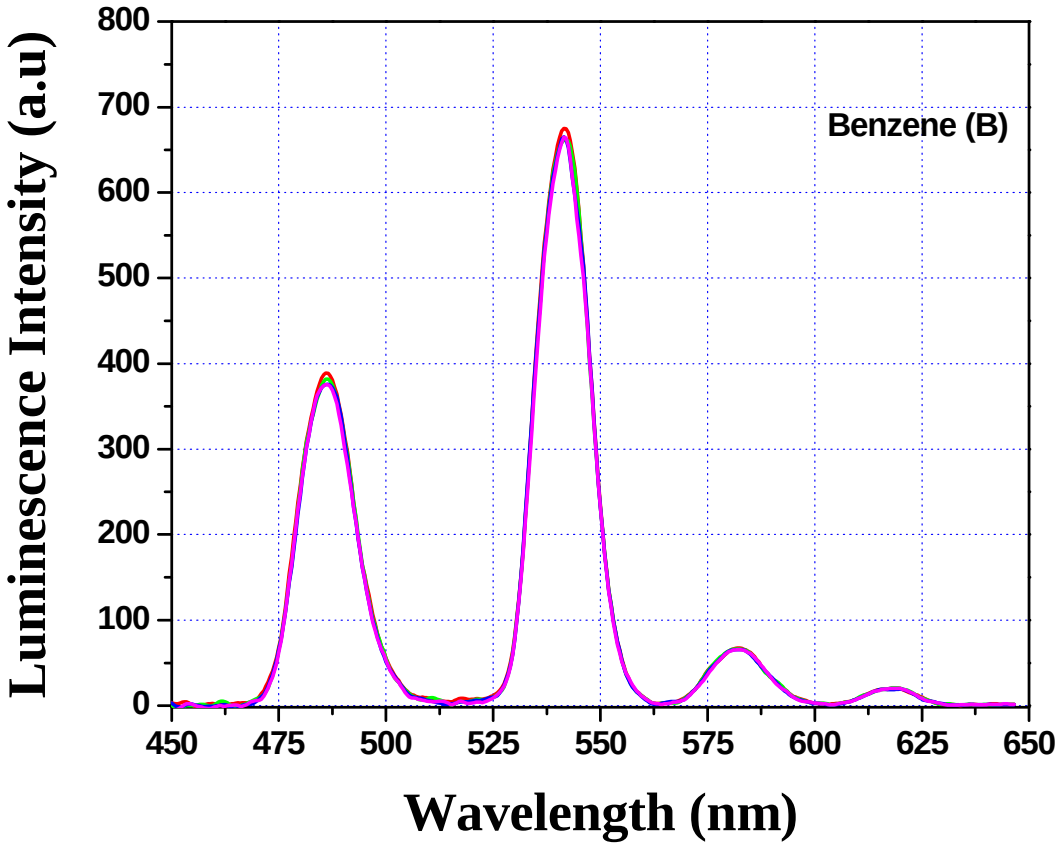

Fig. S14: Emission spectra of **Tb@1'** dispersed in acetonitrile upon incremental addition of benzene solution (0, 20, 40, 60, 80 and 100 μM). λ_{ex} = 225 nm; filter: 430 nm cut-off. Note that all six spectra are superimposed. All the spectra are measured using PerkinElmer LS-55 spectrofluorometer. **Tb@1'** suspension in acetonitrile was prepared by sonicating the mixture of grinded **Tb@1'** and acetonitrile for 1 hour.

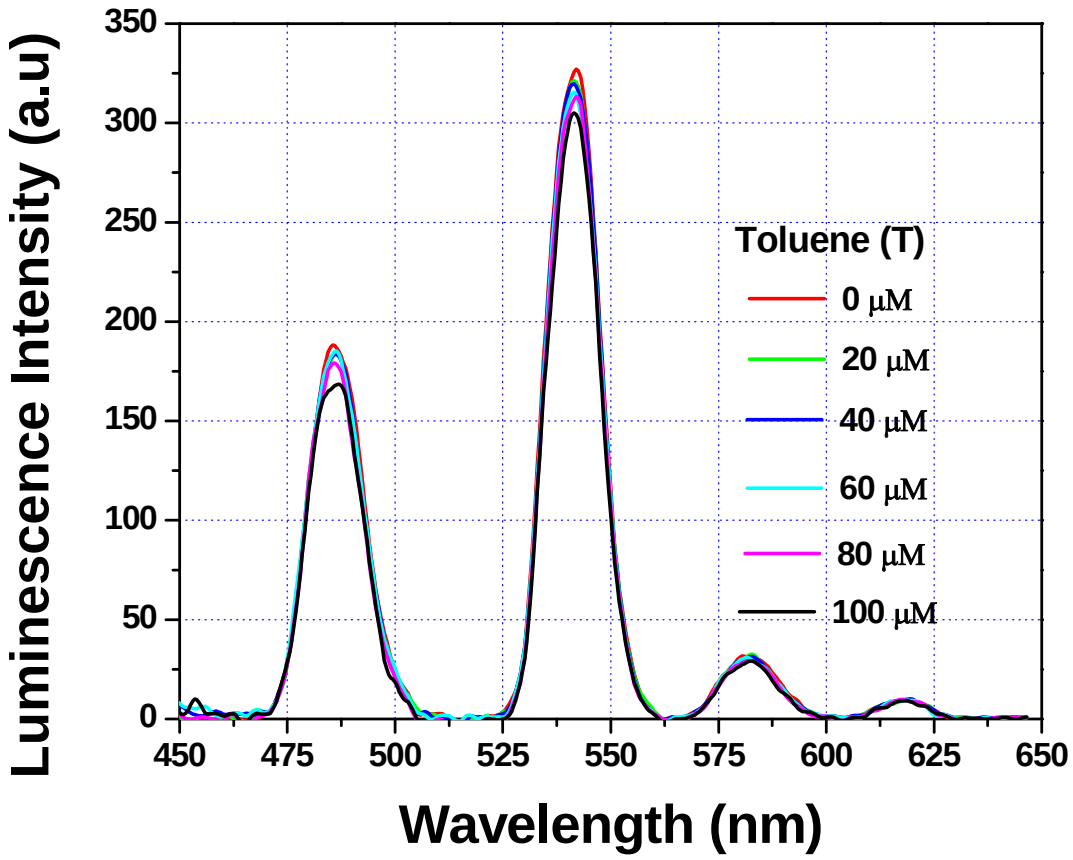

Fig. S15: Emission spectra of **Tb@1'** dispersed in acetonitrile upon incremental addition of toluene solution (λ_{ex} = 225 nm; filter: 430 nm cut-off). The final concentration of toluene in the medium is indicated in the legend. All the spectra are measured using PerkinElmer LS-55 spectrofluorometer. **Tb@1'** suspension in acetonitrile was prepared by sonicating the mixture of grinded **Tb@1'** and acetonitrile for 1 hour.

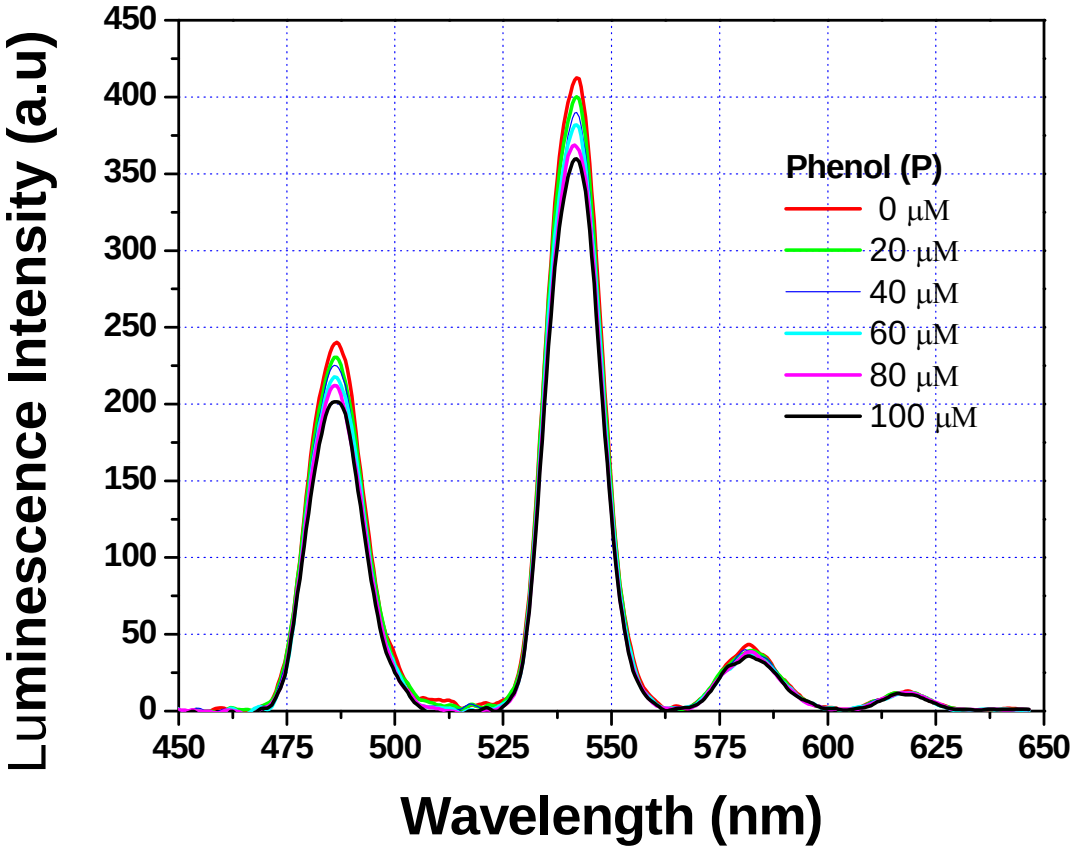

Fig. S16: Emission spectra of **Tb@1'** dispersed in acetonitrile upon incremental addition of phenol solution (λ_{ex} = 225 nm; filter: 430 nm cut-off). The final concentration of phenol in the medium is indicated in the legend. All the spectra are measured using PerkinElmer LS-55 spectrofluorometer. **Tb@1'** suspension in acetonitrile was prepared by sonicating the mixture of grinded **Tb@1'** and acetonitrile for 1 hour.

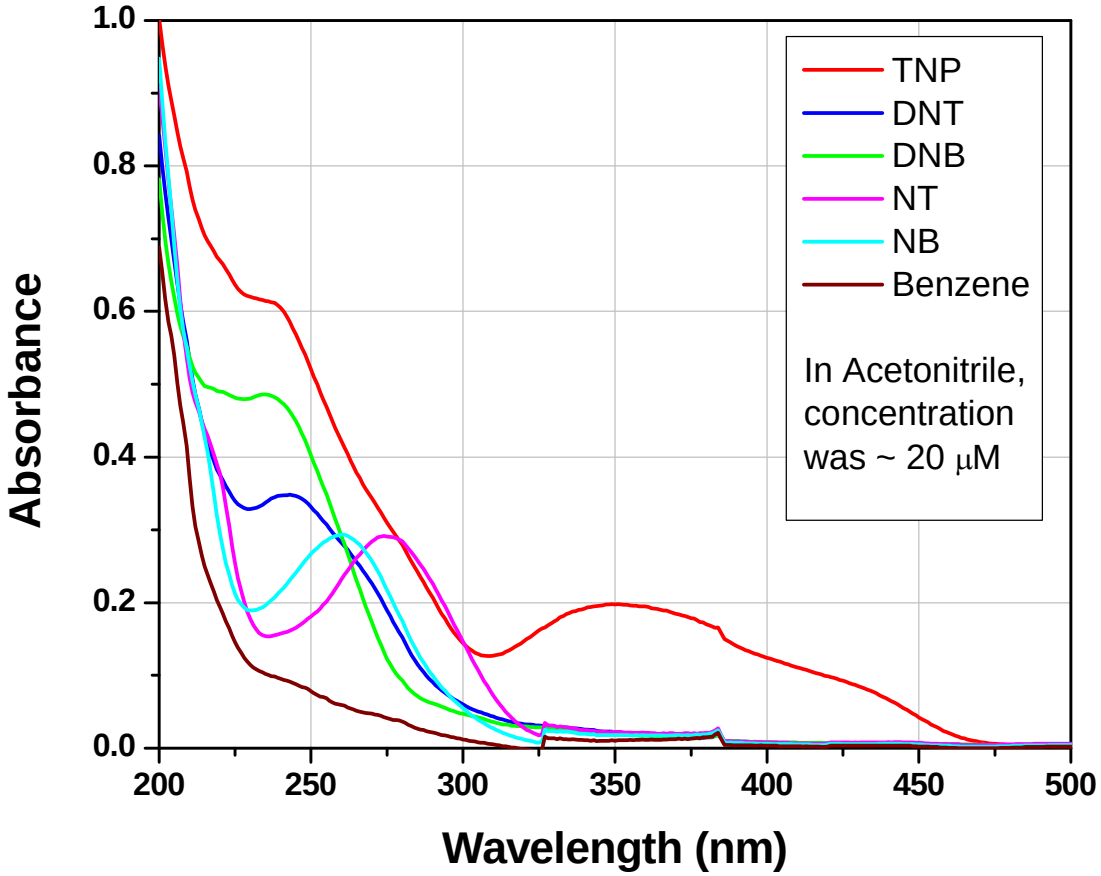

Fig. S17: Absorption spectra of all the six analytes in acetonitrile (Conc. = 20 μM). All the spectra are measured using Shimadzu UV 3101PC spectrophotometer.

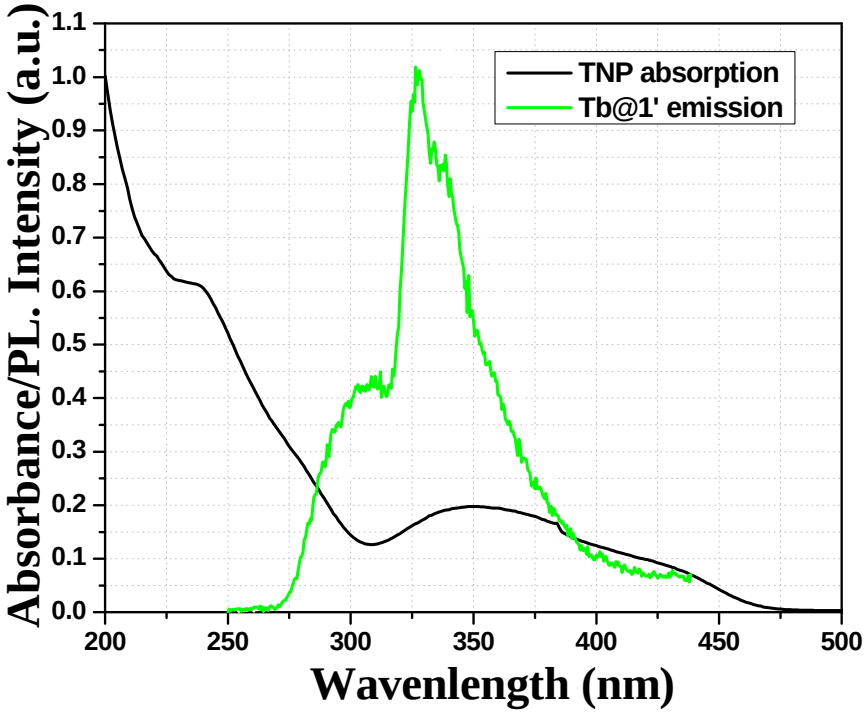

Fig. S18: Absorption spectra of TNP in acetonitrile and ligand based emission spectra of **Tb@1'**. Note the overlap between the emission spectrum of the **Tb@1'** and the longer wavelength absorption band of TNP.

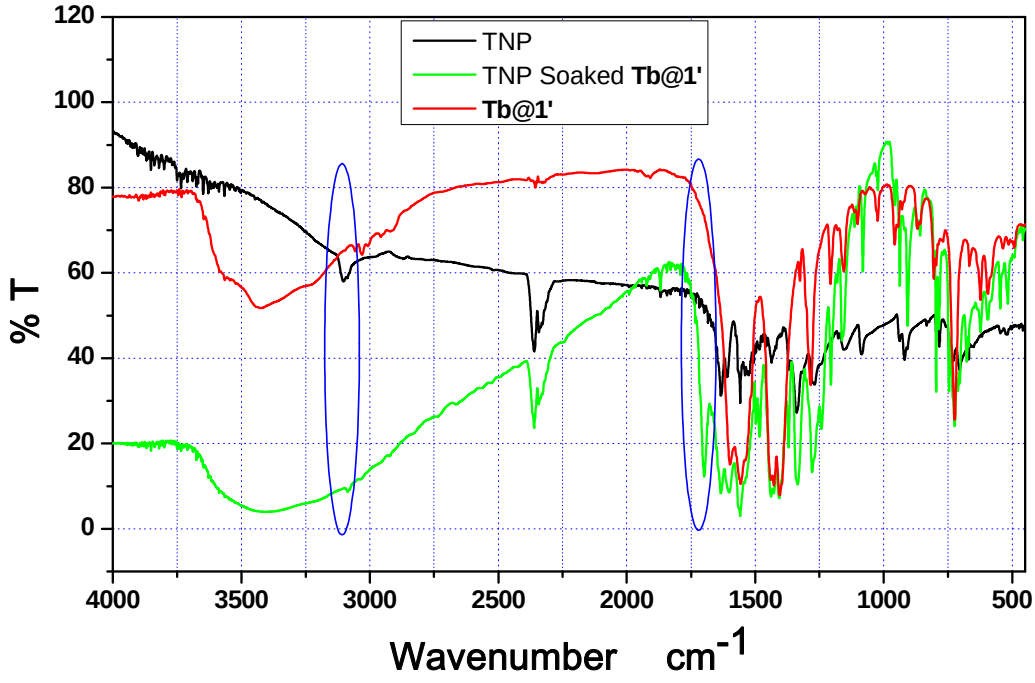

Fig. S19: IR spectra of TNP, TNP soaked **Tb@1'**, and **Tb@1'**. Note the appearance of new peaks at 1700 cm^{-1} in TNP soaked **Tb@1'** indicates hydrogen bonding between carbonyl group of **Tb@1'** and the TNP and the decrease of transmission intensity of CH stretching frequency (~3100 cm^{-1}) of TNP indicate pi-pi interaction between TNP and aromatic ligands (PDA).